

Low-field dependence of the microwave absorption in superconducting $\text{YBa}_2\text{Cu}_3\text{O}_{7-x}$ near T_c

R. Karim, S. A. Oliver, and C. Vittoria
Northeastern University, Boston, Massachusetts 02115

A. Widom
Department of Physics, Northeastern University, Boston, Massachusetts 02115

G. Balestrino,* S. Barbanera, and P. Paroli†
*Istituto di Elettronica dello Stato Solido del Consiglio Nazionale delle Ricerche,
 Via Cineto Romano 42, 00156 Roma, Italy*

(Received 20 April 1988; revised manuscript received 24 October 1988)

Novel microwave absorption and dispersion measurements have been performed on polycrystalline samples and well-characterized single-crystal platelets of high- T_c superconductors $\text{YBa}_2\text{Cu}_3\text{O}_{7-x}$. The results are explained in terms of fluxoids and rapid variation of the penetration depth near and below T_c . The microwave absorption increases as a function of the magnetic field as a result of increase in the surface area of the normal-conducting region. By applying a modulating field in a particular manner and from thermodynamic considerations there are strong indications of energy absorption by fluxoids.

I. INTRODUCTION

Nonresonant microwave absorption experiments provide a valuable technique for investigating high- T_c superconductors. Novel effects associated with granular superconductivity at low fields ($H < 200$ Oe) have been reported.¹⁻⁷ Our experiment was carried out to measure microwave absorption and dispersion near the superconducting transition temperature T_c on bulk material and single-crystal platelets of $\text{YBa}_2\text{Cu}_3\text{O}_{7-x}$ with emphasis on their angular dependence on the applied magnetic fields.

The experimental technique involves the use of a standard electron-spin resonance (ESR) spectrometer at sample temperatures near T_c .⁸ In typical ESR measurements only microwave absorption is measured as the static field (H) is swept through magnetic resonance.⁹ Dispersion measurements are rarely done using this technique, although most ESR systems are capable of performing this measurement. The microwave dispersion is proportional to the shift in cavity frequency which is measured by monitoring the dc voltage output of the automatic-frequency-control (AFC) circuit in the microwave bridge. The AFC dc voltage is proportional to the change in frequency required to "lock" the klystron source frequency to the resonant frequency of the microwave cavity.

Initially, two sets of experiments were performed on the single crystals with different field configurations. In the first set of measurements the dc field (H) is swept while the microwave field (h_{rf}) direction was perpendicular to it. The modulating field (h_m) was applied parallel to H . This is similar to the low-field nonresonant experiment performed by others.¹⁻⁵ From now on this will be referred to as the parallel (\parallel) configuration. In the other magnetically modulated microwave absorption (MMMA) experiment h_m was applied perpendicular to H , but parallel to h_{rf} . We will refer to this experiment as a perpendicular (\perp) configuration. In all of the above experiments the temperature was kept fixed below T_c . In the second

set of experiments H was fixed but T was varied near T_c . The rf magnetic-field source was applied in the platelet plane, the " c " axis being normal to the platelet plane.

We found that in the (\parallel) configuration (d/dH)(power absorbed) as a function of H had a maximum at 10 Oe and the signal was symmetrical about $H=0$. This indicates minimum absorption occurs at $H=0$ and it increases with $|H|$. This contrasts with the reported⁶ maximum absorption at $H \sim 2$ Oe. Hysteresis in the absorption near $H=0$ could possibly shift the extrema in absorption away from $H=0$.

Obviously, for this configuration one should see some sort of change in the signal, (d/dH)(power absorbed), as T is lowered through T_c . This was indeed observed and an almost monotonically decreasing signal, flattening out approximately 6-8 K below T_c was seen. The flat portion of the curve showed some fine structure. The dispersion which is proportional to the change in cavity frequency was observed to show some marked extrema.

The (\perp) configuration experiment exhibited an entirely different behavior as compared to the (\parallel) configuration. First, (d/dH)(power absorbed) versus H showed no change in absorption with respect to H . This remarkable feature can be completely explained by thermodynamic coupling properties of fluxoids.

Second, the temperature experiment in this configuration showed some marked extrema in (d/dH)(power absorbed) near T_c . However, the absorption peaks occurs at temperatures shifted from the (\parallel) configuration.

We interpret our data in terms of existence of fluxoids in these superconductors. In the (\parallel) configuration the absorption as a function of H has a minimum at $H=0$ and increases with $|H|$. This has been explained in terms of weak links⁷ assumed to exist in these high- T_c superconductors. As the field is increased, the number of flux lines or fluxoids also increases (proportionally) the area of the normal-conduction region relative to the superconductive regions. This leads to an increase in the microwave ab-

sorption. The (\perp) configuration shows no dependence of the absorption on H . From thermodynamic considerations of the energy coupling of a fluxoid we conclude the dependence of $Z(\omega + i0^+, H)$ on the modulating field, h_m takes the form $Z = Z(\omega + i0^+, H + h_m \cos\theta)$, where $\cos\theta$ is the cosine of the angle between H and h_m . Later experiments carried out on bulk samples with various angles between H and h_m also fit the predicted angular dependence quite well.

II. SAMPLE CHARACTERIZATION

Single crystals of the high-temperature superconductor $\text{YBa}_2\text{Cu}_3\text{O}_{7-x}$ have been grown by a melt flux method, using as a solvent the eutectic of two of the constituent oxides, namely CuO and BaO, and adding to it a few mol% of Y_2O_3 .¹⁰ The initial composition of the melt, in mol% was Y_2O_3 (3%), BaO (27%), and CuO (70%). Crystal growth was carried out in air, oxygen annealed at 600°C overnight and slowly cooled. Single-crystal platelets of Y-Ba-Cu-O were obtained with surface areas up to several square millimeters, and a typical thickness of 0.1 mm. A crystal of sample dimensions ($1 \times 1 \times 0.05 \text{ mm}^3$) was used in the microwave absorption experiments.

Typical crystals from the melt were characterized by both x-ray diffraction and ac susceptibility measurements. Laue photographs show the surface of the platelet to be normal to the c crystallographic axis. The value of the lattice parameter c was then measured by a single-axis diffractometer using Co $K\alpha$ radiation, from the (0111) symmetric reflection ($2\theta_{\text{Bragg}} = 115^\circ$).

The ac magnetic susceptibility was measured using a superconducting quantum interference device (SQUID) magnetometer as a null detector, at an operating frequency of 80 Hz, and an oscillating field intensity of about 10^{-6} T .¹¹ The magnetic susceptibility variation was recorded as a function of temperature from 125 K down to 4.2 K. Onset of the observed diamagnetic transition was considered to be the onset of superconductivity in the samples.

For the as-grown crystals the value to the lattice parameter along the crystallographic c axis was found equal to $11.724 \pm 0.003 \text{ \AA}$ with a transition temperature of $T_c = 70 \pm 3 \text{ K}$. In addition, the diffraction peak was observed to be quite broad, indicating a spread of c -axis values over the sample. The average lattice value for the c axis was also found to be larger than expected for a 92 K superconducting sample (for example, 11.677 Å in Ref. 12). This behavior indicates a large oxygen deficiency ($x \approx 0.4$) in the sample.¹³ Oxygen was reintroduced into the sample by annealing in 99.99% pure oxygen gas for 48 h at 450°C, and then furnace cooling to room temperature. The effects of this annealing process was a narrowing of the diffraction peaks (indicating an increased and more homogeneous distribution of the oxygen ions over the sample), a decrease in the lattice parameter c to 11.694 Å and an increase in the transition temperature to $85 \pm 3 \text{ K}$. The sample composition after annealing was found to be $\text{YBa}_2\text{Cu}_3\text{O}_{7-x}$. Due to twinning, which microscopically mixes a and b axes, the crystals (even to x-rays) are macroscopically tetragonal, i.e., the twins are so

small that the x rays cannot distinguish that the sample is orthorhombic.

The sample magnetization (M) was measured using a SQUID magnetometer, with magnetic field (H) applied parallel to the c axis at temperatures above and below T_c (7, 80, and 120 K). Above 85 K the sample exhibited typical paramagnetic behavior, as M aligns parallel to, and scales with H . Below 85 K the sample becomes diamagnetic, with dM/dH being zero at 300 Oe and 1 kOe at 80 and 7 K, respectively. We were unable to obtain H_{c2} at any temperature, due to an unavailability of sufficiently high fields. The Meissner effect was found to be of order 11–12% at 7 K. In deducing this value the demagnetizing field in the platelet was taken into account.¹⁴

III. MICROWAVE RESULTS

The microwave absorption and dispersion of a rectangular cavity excited in a TE_{102} rectangular mode tuned at 9.15 GHz was measured. The modulating field h_m was set at 4 G peak to peak (p - p) throughout the experiment and the rf power was held at 2 mW in the microwave cavity.

The superconducting state is affected by the application of external magnetic fields. A fairly linear region of the microwave response with respect to the modulating-field amplitude and microwave-field amplitude was used for the experiments. In all the temperature experiments the samples were zero-field cooled whereas in the field swept experiments the samples were cooled at $H \approx -20 \text{ Oe}$. Figures 1–3 refer to experiments carried out on the single crystal. In Figs. 1(a) and 1(b) the derivative of the microwave absorption as a continuous function of the swept field H is displayed. Figure 1(a) corresponds to the (\parallel) configuration experiment and Fig. 1(b) corresponds to the (\perp) configuration experiment under the same settings of gain, power, and field strength.

Clearly Fig. 1(a) indicates that the derivative of the sample absorption has a maximum near $H = 10 \pm 2 \text{ Oe}$ and is antisymmetrical about $H = 0$. Actually, there is a phase change of π in the detection process about $H = 0$. Thus, the absorption derivative is symmetrical about

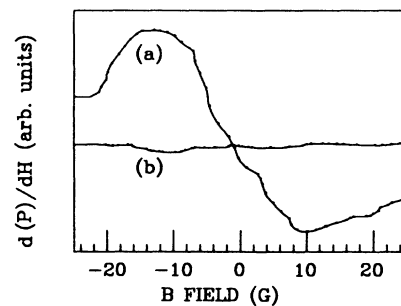


FIG. 1. (a) Field-derivative absorption (P) of a single-crystal high- T_c superconductor is plotted as a function of the swept field H_{dc} in the parallel-configuration experiment. (b) Same sample in the perpendicular-field configuration.

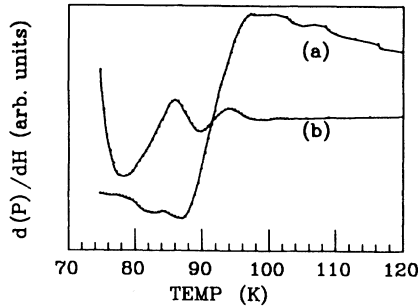


FIG. 2. (a) Field-derivative absorption (P) of the same sample as above is plotted as a function of the temperature in the parallel configuration. The magnetic-field H was fixed at 0 Oe. (b) Same sample in the perpendicular-field configuration. Again H was fixed at 0 Oe.

$H=0$ and the absorption itself has a minimum at $H=0$ and then increases, asymptotically tending to saturation. On the other hand, Fig. 1(b) indicates little change in absorption as a function of H .

The temperature dependence of the microwave absorption and dispersion shown in Figs. 2 and 3 was taken at $H=0$ and $h_m=4$ G (p - p). Variations in the AFC error voltage due to temperature variations of the cavity have been subtracted from the sudden changes of AFC voltages near T_c .

Figure 2(a) displays the absorption derivative as a function of temperature in the (\parallel) configuration. The monotonic decrease in this signal is spread over a range of approximately 6–8 K. Some fine structure is also evident in addition to the main absorption curve. Temperature measurements are accurate to ± 5 K.

Figure 2(b) displays the absorption derivative as a function of temperature in the (\perp) configuration with $H=0$.

Figures 3(a) and 3(b) display the dispersion signals as a function of temperature in the (\perp) and (\parallel) configurations, respectively. The AFC error voltage has been converted to shift in cavity frequency after calibration.

Note that the vertical axes in both plots have been normalized to their values at 120 K and the data have been

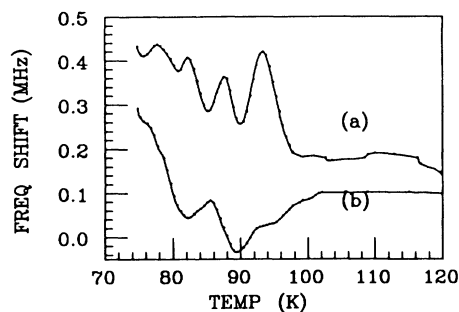


FIG. 3. (a) Shift in the cavity frequency of the same sample as above is plotted as a function of the temperature in the parallel configuration. Again H was fixed at 0 Oe. (b) Same sample in the perpendicular configuration at $H=0$ Oe.

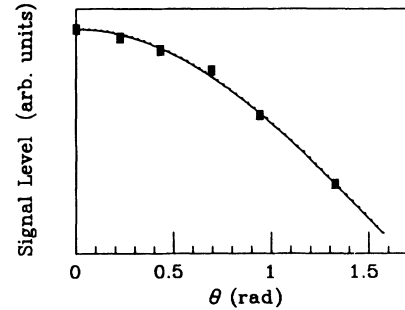


FIG. 4. (a) Absorption-derivative signal level of the bulk sample Y-Ba-Cu-O is plotted as a function of θ , the angle between H and h_m . The solid line represents the calculated fit. The value of H was held constant at 16 Oe.

smoothed by a standard algorithm.

Figure 4 refers to experiments on the bulk sample (approximately 0.3 mm radius). The calculated curve for the absorption derivative and the experimental data points for various angles between H and h_m keeping both $|H|$ and $|h_m|$ constant are compared.

IV. DISCUSSION AND CONCLUSION

A. Field-dependent experiments

Various models have been proposed to explain the low-field absorption in the high- T_c cuprates.^{1–7} A viscous vibration of fluxoids driven by microwave currents (\mathbf{j}) causing the Lorentz force per unit length of a flux quantum (ϕ_0) to be $(1/c)(\mathbf{j} \times \phi_0)$ was found to be the cause of microwave absorption by type-II superconductors.¹⁵ A network of internal Josephson junction currents each reducing the screening of normal electrons by supercurrent according to the “diffraction” expression $I = I_0 \sin(n\pi)/n\pi$, where $n = \phi/\phi_0$, is among the other interesting theories that have been suggested.¹⁶

We have used the phenomenological model of Portis, Blazey, Müller, and Bednorz¹⁷ in order to interpret the experimental data. The salient points of the model are the following. (i) The magnetic-field penetration into the bulk superconductor is assumed to have the form of fluxoids each having the quantum of magnetic flux ϕ_0 and cross-sectional area A_1 . (ii) When these fluxoids thread through the superconductor, they create regions with a normal conductivity σ , inducing a macroscopically averaged resistivity proportional to the number of fluxoids, or equivalently proportional to the magnetic field B ,

$$\rho_n = (A_1 B / \phi_0 \sigma). \quad (1)$$

Equation (1), along with the usual London equation (penetration depth λ), yields the constitutive equation

$$\mathbf{E} = \rho_n \mathbf{J} + (4\pi\lambda^2/c^2)(\partial\mathbf{J}/\partial t). \quad (2)$$

Equation (2) implies that the electromagnetic disturbances within the superconductor propagate with a complex wave vector k ,

$$\frac{1}{k} = -i \left[\lambda^2 + i \left[\frac{\rho_n c^2}{4\pi\omega} \right] \right]^{1/2}. \quad (3)$$

Equation (3) translates into a surface impedance of

$$Z_s = (4\pi\omega/c^2k), \quad (4)$$

or equivalently (for a platelet of thickness d)

$$Z_s(\text{platelet}) \cong \left(\frac{4\pi\omega}{c^2k} \right) \left(\frac{1 - \cos(kd)}{\sin(kd)} \right). \quad (5)$$

Thus, the surface impedance depends on the magnetic field in a complex manner.

To test the above phenomenological model (via the angular dependence of the impedance on the modulating-field direction) one notes that the energy of a single fluxoid in the presence of the modulating-field intensity \mathbf{h} obeys the thermodynamic law

$$\delta U = \frac{1}{4\pi} \int \mathbf{H} \cdot \delta \mathbf{B} d^3r, \quad (6)$$

which for a single fluxoid thread implies

$$\delta U_{\text{fluxoid}} = \frac{\phi_0}{4\pi} \int \mathbf{h}_m \cdot d\mathbf{l} = \frac{\phi_0}{4\pi} \int \cos\theta h_m dl, \quad (7)$$

where θ is the angle between the fluxoid thread direction (length element) $d\mathbf{l}$ and the modulating-field \mathbf{h}_m .

The Poynting theorem relates the energy of the fluxoids to the surface impedance and in terms of the coarse-grained average (over many fluxoids) the surface impedance obeys [from the coupling in Eq. (7)],

$$Z_s(\mathbf{B}, \mathbf{h}_m) = Z_s(B, h_m \cos\theta), \quad (8)$$

where θ is now the angle between \mathbf{B} and \mathbf{h} . Equation (8) is the predicted angular dependence of the fluxoid model, at least in the regime $h \leq B$. In Figs. 1 and 4, Eq. (8) is indeed verified for the angles $\theta=0$ and $\theta=90^\circ$ for the single crystal and for various angles using the bulk sample of Y-Ba-Cu-O.

It seems strange that $H_{c1} \approx 300$ Oe at 80 K, and yet fluxoids are assumed to penetrate by applying a field ~ 10 Oe. However, the latter agrees with Gammel *et al.*,¹⁸ who see fluxoids in Y-Ba-Cu-O cooled in a 13-Oe field.

B. Temperature-dependent experiments

The difference in the temperature dependence of (d/dH) (power absorbed) in the (\parallel) and (\perp) configuration can be explained on the crystal anisotropy and platelet dimensions which will considerably affect the geometrical shape of the fluxoids formed. The rapid variation of the penetration depth near T_c is also a factor to be considered. As can be seen from Eq. (3) the propagation constant k can easily have some contribution from λ at temperatures very close to T_c .

The dispersion curves show some similarity in structure in the (\parallel) and (\perp) configuration, but the absorption peaks are slightly shifted from each other with respect to temperature.

The absorption derivative may be interpreted as a measure of the number of fluxoids trapped as a function of temperature. This implies hysteretic effects as a function of field as observed by us and in Ref. 17.

For the (\parallel) configuration the nature of absorption below T_c is simply understood from the fact that above T_c there are no fluxoids so there is maximum absorption. Below T_c the absorption decreases. Thus, as the temperature is varied from above to below T_c one would indeed expect a change in the MMMA signal. For the (\parallel) configuration this differential in absorption depends on the anisotropy of fluxoid formations (as a function of the direction of H) or simply that there is absorption in the superconducting region as well below T_c . We find that MMMA signal strengths for H parallel and perpendicular to the c axis to be within 15%, eliminating the anisotropy concept. We conclude that in the (\perp) configuration microwave absorption occurs in the superconducting regions rather than in the fluxoid region.

ACKNOWLEDGMENT

This work was partially supported by Progetto Strategico Materiali Superconduttori ad Alta Temperatura Critica of Centro Nazionale delle Ricerche and Sanders Associates superconducting program.

*Also at Dipartimento di Fisica, Universita di Salerno, I-84100, Salerno, Italy.

†Also at Dipartimento di Ingegneria Meccanica, Universita di Roma II, Via O. Raimondo, I-000173 Roma, Italy.

¹C. Rettori, D. Davidov, I. Belaish, and I. Felner, Phys. Rev. B **36**, 4028 (1987).

²S. V. Bhatt, P. Ganguly, T. V. Ramakrishnan, and C. N. R. Rao, J. Phys. C **20**, L559 (1987).

³D. Shaltiel, J. Genossar, A. Grayevsky, Z. H. Kalman, B. Fisher, and N. Kaplan, Solid State Commun. **63**, 987 (1987).

⁴R. Durny *et al.*, Phys. Rev. B **36**, 2361 (1987).

⁵M. D. Sastry, A. G. I. Dalvi, Y. Babu, R. M. Kadam, J. V. Yakmi, and R. M. Iver, Nature **330**, 49 (1987).

⁶K. W. Blazey, K. A. Müller, J. G. Bednorz, and W. Berlinger, Phys. Rev. B **36**, 7241 (1987).

⁷K. A. Müller, M. Takashige, and J. G. Bednorz, Phys. Rev. Lett. **58**, 1143 (1987).

⁸R. Karim, S. A. Oliver, C. Vittoria, G. Balestrino, S. Barbanera, and P. Paroli, J. Superconductivity **1**, 81 (1988).

⁹See, for example, C. Kittel, *Introduction to Solid State Phys-*

ics, 6th ed. (Wiley, New York, 1986).

¹⁰G. Balestrino, S. Barbanera, and P. Paroli, J. Cryst. Growth (to be published).

¹¹S. Barbanera, M. G. Castellano, and V. Foglietti (unpublished).

¹²R. J. Cava, B. Batlogg, R. B. VanDover, D. W. Murphy, S. Sunshine, T. Siegrist, J. P. Remeika, E. A. Rietman, S. Zahrusk, and G. P. Espinosa, Phys. Rev. Lett. **58**, 1676 (1987).

¹³A. Ono, Jpn. J. Appl. Phys. **26**, L1223 (1987).

¹⁴L. D. Landau, E. M. Lifshitz, and L. P. Pitaevskii, *Electrodynamics of Continuous Media*, 2nd ed. (Pergamon, Oxford, 1984).

¹⁵For a review, see C. G. Kuper, *The Theory of Superconductivity* (Oxford Univ. Press, London, 1968), Chap. 7.

¹⁶A. Dulcic *et al.*, Phys. Rev. B **38**, 5002 (1988).

¹⁷A. M. Portis, K. W. Blazey, K. A. Müller, and J. G. Bednorz, Europhys. Lett. **5**, 467 (1988).

¹⁸P. L. Gammel *et al.*, Phys. Rev. Lett. **59**, 2592 (1987).